Journal of Electroceramics, 13, 637–644, 2004

Impedance Spectroscopy on Solids: The Limits of Serial Equivalent Circuit Models

J. FLEIG

Max-Planck-Institute for Solid State Research, Heisenbergstr. 1, 70569 Stuttgart, Germany

Submitted January 14, 2003; Revised October 10, 2003; Accepted October 14, 2003

Abstract. Impedance spectroscopic data obtained on solids are often interpreted in terms of serial equivalent circuit models. In these models each relaxation process in a spectrum is usually related to exactly one transport or reaction process, i.e. to one sample region (e.g. bulk, grain boundary, electrode) or reaction step. These quasi-one-dimensional, serial models implicitly assume frequency-independent current lines. In this contribution it is shown by finite element calculations that in real systems current lines are often frequency-dependent and that the current passes different sample regions at different frequencies. Several effects such as additional semicircles in the complex impedance plane or non-ideal impedance arcs result from frequency-dependent current lines and cannot be understood in terms of serial (quasi-one-dimensional) equivalent circuit models. In particular, it is discussed that (a) one and the same transport process can be reflected in two or even more impedance arcs and (b) that an arc in the impedance plane can depend on more than one transport process (e.g. charge transport in the bulk and across grain boundaries) even if the dielectric relaxation times of the corresponding sample regions (e.g. bulk and grain boundary) are distinctly different.

Keywords: impedance spectroscopy, grain boundary, electrode, relaxation process

1. Introduction

Impedance spectroscopy is a frequently used tool employed in electroceramics. Numerous impedance studies have dealt with, for example, the investigation of grain boundary properties or the characterization of electrode processes in fuel cells or sensors. Mostly, the measured impedance spectra are analyzed in terms of serial equivalent circuits whose elements are correlated with sequential transport or reaction processes, e.g. transport in the bulk, transport across grain boundaries and electrode phenomena. Such a simple serial analysis, however, implicitly assumes that the current passes identical sample regions for all frequencies and, hence, that the current lines in a specimen are frequency-independent. This assumption is, for example, justified in the case of an idealized material with cubic-shaped grains, uniform grain boundaries and uniform electrodes (brick layer model [1–3]). However, in real electroceramics the following question arises: are current lines in materials frequency-independent or does the current change its path with changing frequency thus probing different parts of the sample at different frequencies? If the latter is true, simple serial equivalent circuit models might lead to serious misinterpretations. In several publications the author demonstrated that frequency-dependent current lines are quite common in electroceramic materials and can complicate the impedance analysis [2, 4–10]. In this contribution the general features associated with frequency-dependent current lines are discussed by means of different examples. In particular, it is shown that—in contrast to simple serial models- a certain number of (more or less overlapping) arcs in the complex impedance plane is not necessarily correlated with the same number of transport or reaction processes involved. All results were obtained by solving $\mathrm{div}(\mathrm{grad}\,\varphi) = 0$ (φ = electrical potential) for model systems using the finite element software FLUXEXPERT (Simulog). More computational details have been reported elsewhere [2, 4, 5].

E-mail: j.fleig@fkf.mpg.de

2. The Basic Effects

2.1. An Additional Impedance Arc

In sintering processes of electroceramic materials, inhomogeneities are more the rule than the exception and grain boundaries in one and the same polycrystal can easily differ in terms of structure and chemistry [11–15]. It is not surprising that such inhomogeneous grain boundary properties lead to a distortion of the corresponding grain boundary impedance arc [6, 7]. However, a further phenomenon can result from spatially varying grain boundary properties. Let us, for example, consider a polycrystal with approximately 1/3 of the grain boundaries being completely insulating while all other grain boundaries do not exhibit a significant resistance and thus can be neglected. The resulting inhomogeneous dc potential distribution shows that the current by-passes the insulating grain boundaries (Fig. 1(a)). Consequently, the dc resistance of such a sample is a pure bulk resistance and is not influenced by the transport across grain boundaries (insulating inclusions yield the same effect). An increase in frequency, however, leads to a capacitive "opening" of the insulating grain boundaries and the current lines change. At high frequencies all grain boundaries are dielectrically highly conductive and a completely homogeneous potential distribution results (Fig. 1(b)); the corresponding resistance is that of a single crystal.

This shows that at different frequencies current may pass through different sample regions. However, since for all frequencies transport of free charge carriers

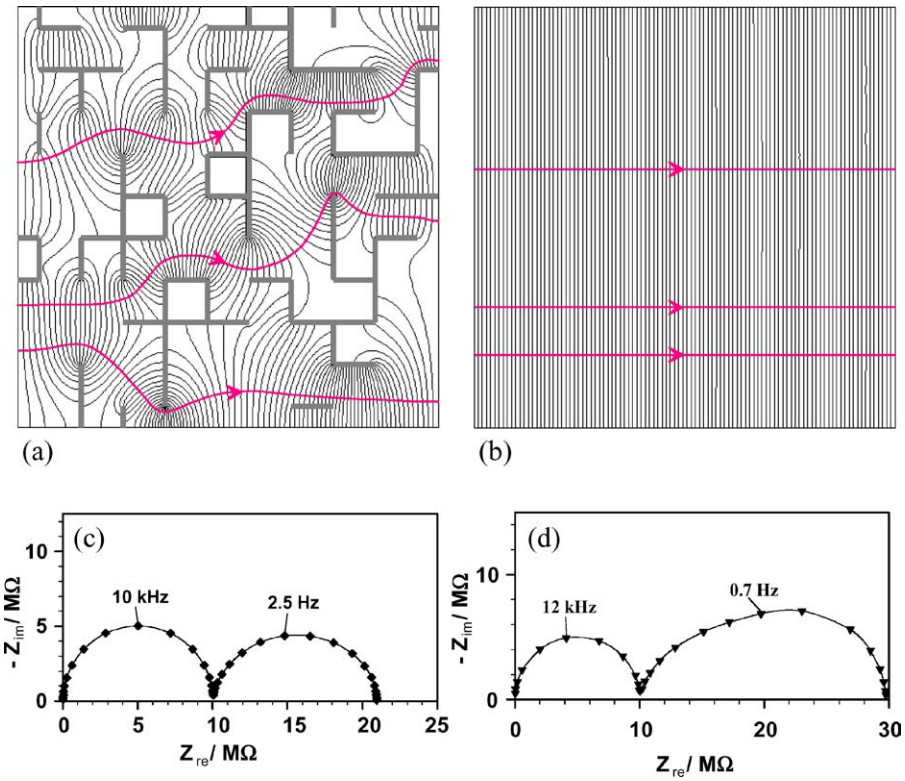

Fig. 1. (a) Calculated dc potential distribution in a square polycrystal consisting of 10×10 grains. Approximately one third of all grain boundaries are completely insulating (dark grey) while all other grain boundaries (not shown) exhibit bulk conductivity and hence are negligible. The voltage drop between two neighboring equipotential lines is one hundredth of the applied voltage; the sketched current lines indicate the current detours which increase the bulk resistance (2D bulk conductivity $= 10^{-7}$ S, grain boundary thickness $= 1$ nm) . (b) Homogeneous potential distribution at frequencies larger than the relaxation frequency of the bulk. (c) Corresponding calculated impedance spectrum. (d) Calculated impedance spectrum for another spatial distribution of blocking grain boundaries.

occurs in the bulk only, a simple model, where one transport process corresponds to one semicircle would predict exactly one arc in the impedance plane. This has been disproved by our calculations: an additional arc appears at low frequencies (Fig. 1(c)) and even though it looks like a distorted grain boundary semicircle its resistance only reflects the difference between the dc bulk resistance (including detours) and the high-frequency bulk resistance (without detours). Hence, the resistance of the low-frequency arc does not contain any information on grain boundary conductivities. The size and the shape of the additional low-frequency arc depends on the exact spatial distribution of the blocking grain boundaries. Even two (overlapping) low frequency semicircles may appear for certain distributions thus pretending two additional relaxation processes though only charge carrier transport in the bulk plays a role (Fig. 1(d)).

These calculations demonstrate (i) that not only additional transport processes but also frequency-dependent current lines can yield additional arcs in the complex impedance plane ("switching current line arcs") and (ii) that from the occurrence of two semicircles it cannot be concluded that two different transport or reaction processes are involved. Hence, frequency-dependent current lines yield impedance effects that do not exist in 1D considerations and conventional serial models can therefore lead to severe misinterpretations of impedance data. However, there is a way to distinguish such apparent "grain boundary semicircles" from true grain boundary effects. Since the resistance of a switching current line arc is completely bulk determined, the same temperature, dopant and partial pressure dependencies can be expected for the high- and low-frequency arcs. A variation of these external parameters can thus reveal whether a switching current line arc exists or not.

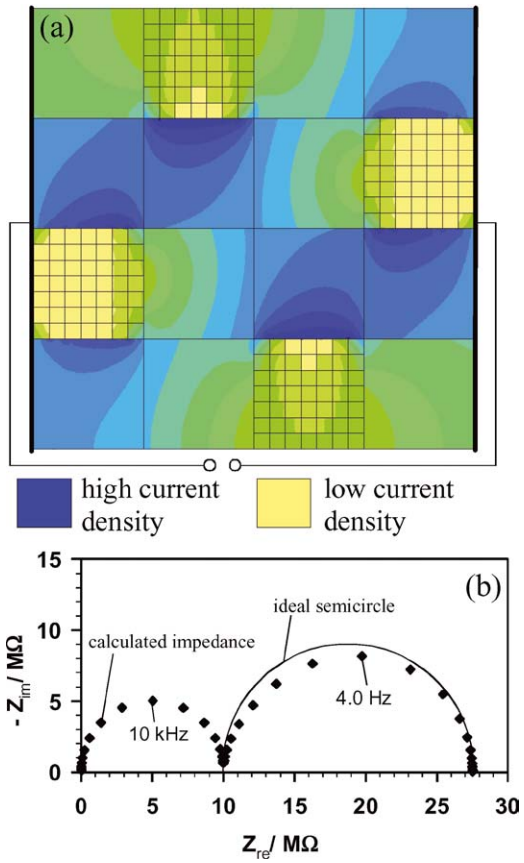

Fig. 2. (a) Magnitude of the dc current density in an artificial 2D microstructure representing the case of an inhomogeneous grain size distribution (agglomeration of smaller grains) for a 2D bulk conductivity σ_{bulk} of 2×10^{-7} S, grain boundary conductivity $\sigma_{gb} = 4 \times 10^{-11}$ S, and grain boundary thickness = 2.8 nm. (b) Calculated impedance spectrum for the same microstructure ($\sigma_{bulk} = 10^{-7}$ S, $\sigma_{gb} = 4 \times 10^{-11}$ S, grain boundary thickness = 2.8 nm) and an ideal semicircle for comparison demonstrating the distortion of the grain boundary arc.

2.2. *A Depressed Grain Boundary Semicircle Despite Uniform Grain Boundary Properties*

Another effect of frequency-dependent current lines can be illustrated for a sample with identical, moderately resistive grain boundaries and spatially varying grain sizes. In Fig. 2(a) a model sample exhibiting an inhomogeneous grain size distribution is shown. The sample consists of 12 large square grains and 4 agglomerates with 49 small grains each. Even though all grain boundaries exhibit identical properties, a non-ideal low frequency semicircle results for such a polycrystal (Fig. 2(b)). A fit of the left half of the low-frequency arc using a constant phase element (impedance $Z_Q = Q^{-1}(i\omega)^{-\beta}$) in parallel with a resistor yields a β-value of 0.916 while the right half results in $\beta = 0.99$. This distortion of the semicircle is not due to a distribution of relaxation frequencies (as one might conclude in a conventional analysis) but is instead a consequence of the frequency dependence of the current lines. For low frequencies the current avoids excess grain boundaries and thus partly bypasses the agglomerates of small grains (Fig. 2(a)). For high frequencies (of the order of the bulk relaxation

frequency), on the other hand, all interfaces are dielectrically short-circuited and a homogeneous current distribution results. This frequency-dependent switching of the current lines leads to the non-ideality of the low frequency semicircle. However, this effect cannot solely account for severely depressed grain boundary semicircles often found in experiments (say β-factors below 0.9) and it is likely that in such cases both distributions of relaxation times and frequency-dependent current lines play together in distorting the grain boundary arc.

2.3. *Grain Boundary Semicircles Being Influenced by the Bulk Conductivity*

An artificial though very illustrative example reveals a further phenomenon related to frequency-dependent current lines. Fig. 3a shows a grain boundary pattern with zig-zag grain boundaries. As one might expect, the impedance spectrum consists of two semicircles. However, the diameter of the low-frequency arc (R_2) depends on both grain boundary and bulk conductivity (Fig. 3(b)). In order to understand this behavior let us consider the dc potential distribution (Fig. 3(c)). The current partly avoids the additional hindrance of a zig-zag grain boundary and this leads to the bulk-dependent grain boundary semicircle.

The number of grain boundaries being passed by the current depends on the bulk conductivity. This results from the interplay of two effects: detours can lower the resistance associated with the crossing of grain boundaries but they also lead to longer current paths and thus enhance the resistance in the bulk. Depending on the ratio of bulk to grain boundary conductivity ($\sigma_{bulk}/\sigma_{gb}$), detours are therefore more or less pronounced. A detour around a zig-zag grain boundary is "easy" for high bulk conductivities (compared to σ_{gb}) and in the limit of very large σ_{bulk} the zig-zag grain boundary is indeed completely avoided and does not carry any current. For small bulk conductivities, however, detours would significantly increase the resistance in the bulk and are thus largely avoided; a nearly homogeneous potential distribution results and the current crosses the zig-zag grain boundary. As a consequence, the number of grain boundaries being passed by the current and thus also the diameter of the low frequency arc (R_2) depends on the bulk conductivity.

There is a second reason for R_2 being σ_{bulk}-dependent: the additional bulk resistance due to current detours contributes to the low-frequency rather than to the high-frequency semicircle in the impedance spectrum. This can again be understood from the frequency dependence of the current lines. For high frequencies all grain boundaries are dielectrically short-circuited and the potential distribution is homogeneous for the

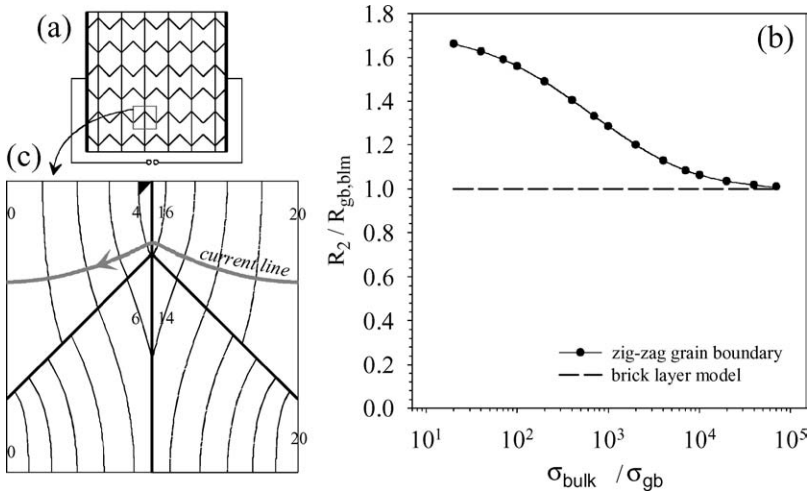

Fig. 3. (a) 2D polycrystalline sample with zig-zag grain boundaries. (b) Grain boundary resistance R_2 normalized to the resistance for square grains ($R_{gb,blm}$) in dependence of the bulk conductivity (normalized to the grain boundary conductivity). (c) Calculated dc potential distribution in a basic element for $\sigma_{bulk} = 10^{-4}$ S, $\sigma_{gb} = 10^{-7}$ S and a grain boundary thickness of 10^{-3} times the size of the basic element. The numbers indicate the potential in mV for an applied voltage of 20 mV.

entire high frequency semicircle. Consequently, the high frequency arc still reflects the ideal bulk properties and is not affected by grain boundary microstructures. The additional bulk resistance due to the detours plays a role only at low frequencies and therefore contributes to R_2. This bulk-dependent grain boundary arc is again an effect that cannot be expected from a simple serial model. In the case of a serial analysis each transport process leads to exactly one semicircle while in the present case conductivities of two transport processes (e.g. grain boundary and bulk) can influence the same impedance arc even though the dielectric relaxation times of the corresponding sample regions (bulk and grain boundary) are distinctly different. (It should be mentioned that the example in Section 2.2 exhibits the same feature.) The dependence of the so-called "grain boundary resistance" R_2 on σ_{bulk} also affects the temperature dependence of R_2. It is shown in more detail in Ref. [7] that the activation energy calculated from R_2 can deviate from the true grain boundary activation energy and that deviations from an Arrhenius behavior may occur.

3. Further Examples

3.1. Partially Wetting Grain Boundary Phases

Grain boundaries are often laterally inhomogeneous in the sense that conducting as well as insulating interface regions are present. To give two examples: (i) solid grain boundary phases may partially wet the grains and lead to a diminished grain-to-grain contact; (ii) nanopores along grain boundaries cause imperfect contacts between two grains. Here we consider a sample consisting of cubic grains with all grain boundaries being partially covered by an insulating phase of constant thickness (Fig. 4); circular grain-to-grain contacts with negligible transfer resistance are assumed. The calculated dc and high frequency potential distributions in a cross section of a grain are given in Fig. 4(c) and (d). In the dc case (Fig. 4(c)), current constriction occurs close to the circular contact while for frequencies of the order of the bulk relaxation frequency a homogeneous potential and current distribution results (Fig. 4(d)). Two semicircles appear in the complex impedance plane

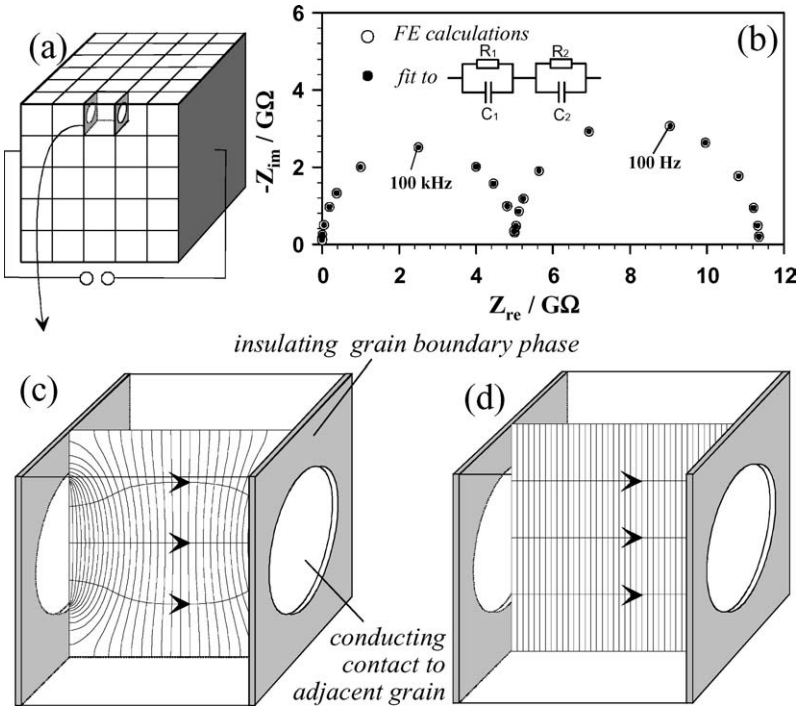

Fig. 4. (a) Polycrystal consisting of cubic grains with circular grain-to-grain contacts (white) and an insulating grain boundary phase of constant thickness (grey). (b) Impedance spectrum of a single grain (see c, grain size = 2 μm, $\sigma_{\text{bulk}} = 10^{-6}$ S/cm) and the equivalent circuit used to fit the impedance data. (c) Calculated dc potential distribution (equipotential lines) in a cross section of a single grain and sketched current lines. (d) Calculated potential distribution and three current lines at the dielectric relaxation frequency of the bulk.

(Fig. 4(b)). The high-frequency semicircle is independent of the detailed grain-to-grain contact geometry while the low frequency semicircle decreases for increasing contact area.

The frequency dependence of the potential distribution again provides the key to understand the low frequency semicircle. For high frequencies, the insulating grain boundary phase is capacitively conductive and thus negligible. The resulting homogeneous current distribution holds good for the entire high frequency semicircle and the diameter of this arc (R_1) equals the "ideal" (quasi one-dimensional) bulk resistance. The dc resistance is also a bulk resistance since the entire dc voltage drops in the bulk. However, it includes the contribution caused by the current constriction near the contact and is thus larger than R_1. In other words, the low frequency arc is again a switching current line semicircle and reflects the transition from the "ideal" bulk resistance R_1 to the increased dc bulk resistance ($R_1 + R_2$) caused by the more and more blocking character of the capacitance of the insulating phase for decreasing frequencies. A more detailed discussion of the impedance of polycrystalline materials with partially wetting grain boundaries or incomplete grain-to-grain contacts can be found in Ref. [2]. Therein earlier intuitive models dealing with imperfect contacts [16–19] are evaluated and it is shown that, even though a serial equivalent circuit (see Fig. 3(b)) is appropriate to fit the spectra, it cannot be interpreted in the conventional (one-dimensional) way via two series regions.

3.2. *Impedance Effects Due to Geometrically Imperfect Electrodes*

Paste electrodes as well as arc- or flame-sprayed and screen-printed electrodes consist of micrometer- or nanometer-sized particles and thus lead to inhomogeneous electrode/solid interfaces. As a kind of prototype of such inhomogeneous electrodes we consider a model interface consisting of circular, ideally ohmic contact areas and thin insulating air gaps. A cross-section of such an electrode is shown in Fig. 5(a). In the dc case the current flows to the contacted areas (Fig. 5a) and the corresponding dc resistance of the sample is thus enhanced due to the current constriction close to the contact spots. Since the entire voltage still drops in the bulk of the model sample, the resulting resistance is a bulk resistance and solely determined by σ_{bulk} and the contact geometry. However, if an ac voltage of sufficiently high frequency is applied, the air gaps at the sample/electrode interface become dielectrically conducting and the resulting potential distribution is almost homogeneous as in the case of an ideal electrode contact (Fig. 5(b)). The corresponding resistance is the ideal 1D bulk resistance of the sample.

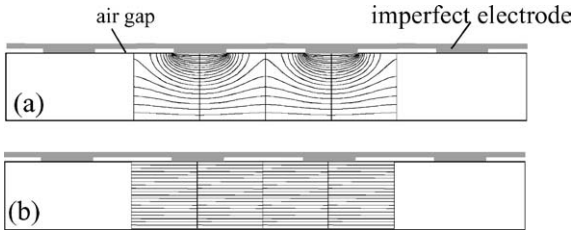

Fig. 5. (a) Cross-section of a 3D model sample with a geometrically imperfect electrode (circular current-carrying contacts and insulating air gaps) and calculated dc potential distribution (equipotential lines) in a part of the sample; (b) ac potential distribution for frequencies of the order of the bulk relaxation frequency. For the sake of clarity the sketched thickness of the air gaps is much larger than the thickness used in the calculation (10^{-3} sample thickness). In both potential distributions the difference between two equipotential lines is U/20 with U being the applied voltage.

Hence, a situation as for partially wetted grain boundary phases results: the bulk resistance changes with frequency and a switching current line semicircle appears in the complex impedance plane. The diameter of the low frequency arc reflects the additional bulk resistance R_2 due to the current constriction close to the contact spots and an interpolation formula for R_2 is given in Refs. [5, 22]. The high frequency semicircle, on the other hand, corresponds to the bulk resistance and bulk capacitance that would result for an ideal and complete electrode contact. Consequently also for inhomogeneous electrodes correct bulk properties can be deduced from impedance measurements.

In order to decide whether a true electrode process or current constriction is the physical origin of an additional semicircle, temperature and dc bias-dependent measurements are recommended. Firstly, the resistance of a low-frequency arc due to current constriction exhibits bulk activation energy, at least if the contact geometry is temperature-independent. Secondly, electrode processes are in general strongly bias-dependent while a switching current line semicircle is bias-independent. Further information, e.g. on the relation between the low frequency capacitance and the geometrical capacitance of the air gaps, the relaxation time of the low frequency arc and the effects of

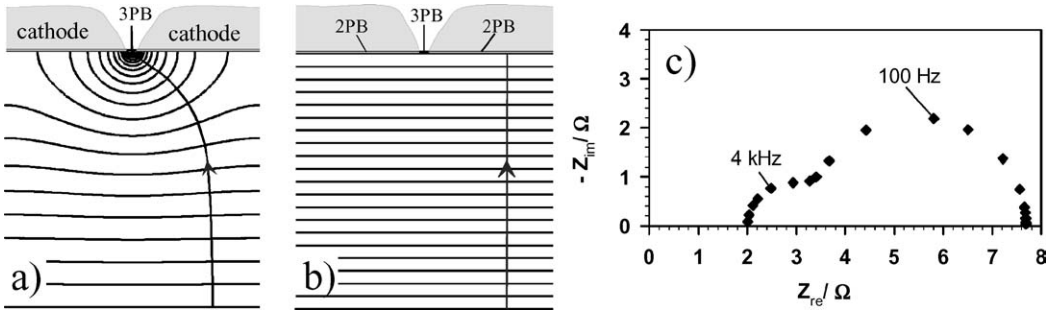

Fig. 6. (a) dc equipotential lines and one current line in a prototype cathode that represents the main qualities of many solid oxide fuel cell cathodes: an electrochemically active three-phase-boundary (3PB) and inactive two-phase-boundaries (2PB) between cathode particles and electrolyte. (b) Corresponding homogeneous high frequency potential distribution. (c) Example of a resulting impedance spectrum.

a varying air gap thickness are given in Refs. [5, 8]. Experimental evidence for such switching current line semicircles at electrodes can, for example, be found in Refs. [9, 23–25].

3.3. *Additional Low-Frequency Semicircle for Porous SOFC Electrodes*

Gas electrodes in electrochemical cells (for example solid oxide fuel cells or gas sensors) have to be porous in order to supply gaseous species to the electrochemically active sites. Impedance spectra of such porous gas electrodes frequently exhibit more than one "electrode semicircle" in the complex impedance plane and one might suppose that complicated electrode mechanisms are required to interpret such results. The following 2D example shows, however, that two low-frequency semicircles can already develop for the most simple reaction model. We assume a cathode where only in the so-called three phase boundary (3PB) area the ionic current in the electrolyte is transferred into an electronic current in the electrode. Hence, the dc current in the electrolyte has to flow to the 3PB area where current density (j) and electrode potential drop ($\Delta\varphi$) associated with the electrochemical reaction are related via $j = (Y + i\omega C)\Delta\varphi$ with Y, C being an admittance and capacitance per area (Fig. 6(a)). (For the sake of simplicity, the distance between two electrode particles is assumed to be so small that the electrochemically active 3PB area covers the entire electrolyte/gas interface (Fig. 6)). However, the ion-blocking two phase boundary (2PB) between electrode and electrolyte can be considered as a kind of double layer capacitor with area-specific capacitance of about 10–30 μF/cm^2. Hence, the 2PB becomes dielectrically permeable at higher frequencies and the current constriction disappears (Fig. 6(b)). The role of the 2PB is similar to that of the air gaps in the case of an imperfect electrode (Section 3.2) though the 2PB capacitance per area is usually much larger than that of air gaps at electrodes.

Thus, the dielectric current across the 2PB "short-circuits" the polarization impedance of the electrochemical reaction as well as the additional electrolyte resistance due to current constriction at the 3PB. Consequently, it can be expected that the part of the dc electrolyte resistance that originates from the current constriction plays no role at high frequencies and contributes to the low-frequency impedance. This is confirmed by the calculated spectrum in Fig. 6(c): two low frequency semicircles rather than one electrode arc appear in the complex impedance plane. The smaller arc (at medium frequencies) is caused by the switching of the current lines and thus depends on the bulk conductivity. The larger arc at low frequencies is due to the electrochemical reaction. A simple equivalent circuit to deduce electrochemical and electrical parameters from such an impedance spectrum is discussed in Refs. [4, 10]. This calculation demonstrates that additional "electrode" semicircles in electrochemical experiments are not necessarily caused by complicated electrochemical mechanisms.

4. Conclusions

- Two semicircles in the complex impedance plane are not necessarily connected with two serial transport or reaction processes but can also be caused by

frequency-dependent current distributions (switching current line semicircle).
- A non-ideal semicircle can result from pure geometrical effects and, hence, does not always hint towards a distribution of relaxation times.
- An arc in the impedance plane can depend on two transport processes (e.g. charge transport in the bulk and across grain boundaries) even if the dielectric relaxation times of the corresponding sample regions (e.g. bulk and grain boundary) are distinctly different.
- Additional temperature, bias, partial pressure or dopant dependent measurements may be required in order to identify switching current line semicircles at low frequencies. From high-frequency semicircles, however, correct bulk properties can usually be deduced.

References

1. N. Bonanos, B.C.H. Steele, and E.P. Butler, in *Impedance Spectroscopy*, edited by: (J.R. Macdonald, John Wiley and Sons, New York, 1987), p. 191.
2. J. Fleig and J. Maier, *J. Am. Ceram. Soc.*, **82**, 3485 (1999).
3. J. Maier, *Ber. Bunsenges. Phys. Chem.*, **90**, 26 (1986).
4. J. Fleig, P. Pham, P. Sztulzaft, and J. Maier, *Solid State Ionics*, **113–115**, 739 (1998).
5. J. Fleig and J. Maier, *J. Electroceramics*, **1**, 73 (1997).
6. J. Fleig and J. Maier, *J. Europ. Ceram. Soc.*, **19**, (1999) 693.
7. J. Fleig, *Solid State Ionics*, **131**, 117 (2000).
8. J. Fleig and J. Maier, *Electrochim. Acta*, **41**, 1003 (1996).
9. J. Fleig and J. Maier, *Solid State Ionics*, **85**, 17 (1996).
10. J. Fleig and J. Maier, *J. Electrochem. Soc.*, **144**, L302 (1997).
11. F. Greuter and G. Blatter, *Semicond. Sci. Tech.*, **5**, 111 (1990).
12. M. G. Norton and C.B. Carter, in *Materials Interfaces*, edited by D. Wolf and S. Yip (Chapman & Hall, London, 1992), p. 151.
13. E. Olsson and G. L. Dunlop, *J. Appl. Phys.*, **66**, 3666 (1989).
14. M.A. Gülgün, V. Putlayev, and M. Rühle, *J. Am. Ceram. Soc.*, **82**, 1849 (1999).
15. I. Denk, J. Claus, and J. Maier, *J. Electrochem. Soc.*, **144**, 3526 (1997).
16. J.E. Bauerle, *J. Phys. Chem. Solids*, **30**, 2657 (1969).
17. M. Kleitz, H. Bernard, E. Fernandez, and E. Schouler, Advances in Ceramics, *Science and Technology of Zirconia*, edited by A.H. Heuer und L.W. Hobbs (American Ceramic Society, Washington, D.C., 1981), Vol. 3, pp. 310.
18. M. Kleitz, L. Dessemond, and M. C. Steil, *Solid State Ionics*, **75**, 107 (1995).
19. M.C. Steil, F. Thevenot, and M. Kleitz, *J. Electrochem. Soc.*, **144**, 390 (1997).
20. L.C. DeJonghe, *J. Mat. Sci.*, **14**, 33 (1979).
21. P.G. Bruce and A.R. West, *J. Electrochem. Soc.*, **130**, 662 (1983).
22. J. Fleig and J. Maier, in *Solid Oxide Fuel Cells V*, editors by U. Stimming, S.C. Singhal, H. Tagawa, and W. Lehnert, PV 97-40 (The Electrochem. Soc., Pennington, NJ, 1997), p. 1374.
23. J.-H. Hwang, K.S. Kirkpatrick, T.O. Mason, and E.J. Garboczi, *Solid State Ionics*, **98**, 93 (1997).
24. E. J. Abram, D. C. Sinclair, and A. R. West, *J. Electroceramics*, **7**, 179 (2001).
25. E. Wanzenberg, F. Tietz, D. Kek, P. Panjan, and D. Stöver, *Solid State Ionics*, **164**, 121 (2003).